

Sea Docking Experiment with Vision-based Recognition Using Dual-eye Camera

Kenta Yonemori¹, Myo Myint¹, Mamoru Minami¹, Naoki Mukada¹ and Khin Nwe Lwin¹

¹Graduate School of Natural Science and Technology, Okayama University, Japan

(Tel: 81-86-251-8233, Fax: 81-86-251-8233)

¹pceo8sjx@s.okayama-u.ac.jp

Abstract: Nowadays, AUV is playing an important role for human society in different applications such as inspection of underwater structures (dams, bridges). However, there is limitation for AUV in terms of power, resulting in difficulties for especially long operation in time. To solve this problem, underwater recharging function is one of the solution to enable the AUV to operate for extended periods independently on a surface vessel. In this way, docking operations become essential for applications such as homing under mother ship, catching AUV after operation, and underwater battery recharging. There are many kinds of approaches for docking operation using different sensors and techniques. This paper presents dual-eye vision-based docking system. We conducted sea docking operation using this system in Wakayama Prefecture.

Keywords: Visual Servoing, Remotely Operated Vehicle(ROV), Genetic Algorithm, Docking

1 INTRODUCTION

Nowadays, AUVs are being used in many applications such as underwater cable tracking, sea bottom surveying and inspection of underwater structures (dams, bridges). However, there is limitation for underwater vehicles for operations that take longer duration time than power capacity of underwater vehicles. Even though advanced technology related to power devices provides long operation period, underwater vehicles has to come surface vessel for recharging when operations take couples of days. To overcome this issue, underwater recharging station with docking function has being implemented recently using different kinds of approaches. On the other hand, docking operation has become noble capability of AUVs for advanced applications such as sleeping under mother ship, downloading next target instruction, navigation and intervention using some manipulators. With this motivation, we have developed dual-eye vision-based docking system for underwater battery recharging to extend the operations of AUVs.

The review and survey on visual measurement and control for underwater vehicles is introduced[1]. Many studies on underwater vehicle using visual servoing have been conducted all around the world recently. Some researches are based on the monocular vision [2] and some are using two cameras [3][4]. However, in [3][4], the two cameras were not used for 3D pose estimation. In [5][6], other sensors or landmarks were used in some applications in need of 3D. Most of them [5][6] using different image processing techniques, are relying on the image features. Therefore, the performance of target recognition may degrade when the underwater environment poses difficulties for correct detection of feature points, especially when dealing with dynamic images.

To solve these problems, a visual servoing system as

shown in Fig.1 utilizing Model-based Matching method and Genetic Algorithm(GA) has been proposed [7][8]. The system includes a pair of dual-eye camera and a 3D maker with known shape and colors information. We have succeeded in docking experiments in a pool filled with tap water[9]. However, the evaluation of effectiveness of proposed system in the actual sea area is not sufficient in this environment[9]. Therefore, in order to confirm the effectiveness of proposed system in the actual sea area, docking experiments in which the main task is to insert a docking pole(8×6 [mm]) attached in ROV into the docking hole with diameter of 70 [mm] were conducted in the bay of Wakayama Prefecture. This report describes the details concerning docking experiment of ROV in sea.

2 ROV(REMOTELY OPERATED VEHICLE)

Hovering type underwater vehicle (manufactured by Kowa cooperation) is used as a test bed as shown in Fig.1. Two fixed cameras installed at the front of the vehicle are used for real time pose tracking. In thruster unit, four thrusters with maximum thrust force of 4.9[N] each are controlled to move the vehicle along desired path. The vehicle can dive up to 50 [m] and two LED light sources are also installed on the vehicle. The specification of ROV is shown in Table 1.

3 REAL TIME POSE TRACKING USING STEREO VISION

3.1 Realtime 3D pose estimation

Instead of calculation of absolute position of vehicle and target in docking station, estimated relative pose is input as feedback to the control system. Avoiding to the limitation

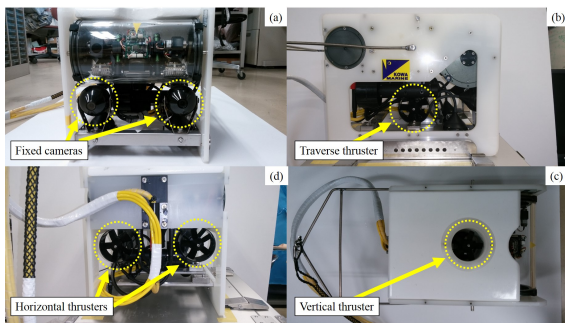


Fig. 1. Photograph of ROV

Table 1. Specification of ROV

Maximum operating depth [m]	50
Dimension [mm]	280(W) × 380(L) × 310(H)
Dry weight [kg]	15
Number of thrusters	2(Horizontal) 1(Vertical), 1(Traverse)
Number of cameras	2(Front, fixed)
Number of LED lights	2(5.8 [W])
Tether cable [m]	200
Maximum thrust force [N]	9.8(Horizontal) 4.9(Vertical, Traverse)

of features based recognition especially wrong mapping corresponding features in images, 3D model-based recognition based on 3D to 2D projection was applied in proposed system. The information of 3D marker that are size, shape, color information are known and defined as model in computer system. Models with different poses are projected to 2D images and compared with captured images from two cameras. Then estimated pose of the best model that is matched totally to the captured images is assumed to be truthful estimated pose for control system. To perform in real time, we used GA with long history and modified as Real-time Multi-step GA for searching the best model. Matching degree is evaluated using fitness function based on voting performance. The detail explanation of fitness function is discussed in [10]. Fig.2 shows the flowchart of Real-time Multi-step GA. Real time pose is estimated for every image with image frame rate of 33 [ms]. Parameters of Real-time Multi-step GA are defined as shown in Table 2.

Table 2. Parameters of Real-time Multi-step GA

Number of genes	60
Pose (Position, Orientation)	Position(x mm, y mm, z mm). Orientation(ϵ_3 deg) around z -axis of Σ_H in Fig.3
Searching space [mm] defined by Σ_H in Fig.3	$\{x,y,z\}=\{\pm 400, \pm 400, \pm 200\}$
Control period [ms]	33
Number of gene evolution [times/33ms]	9
Evolution strategy	Elite preservation

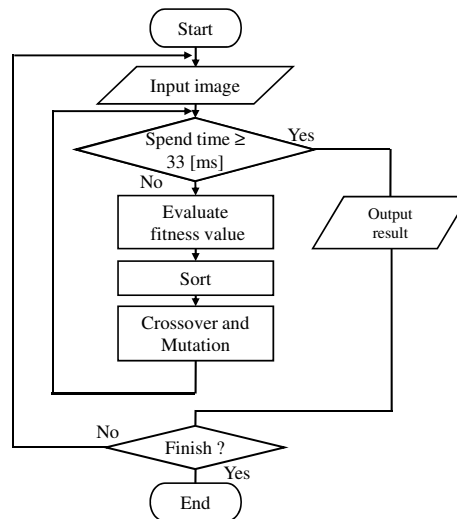


Fig. 2. Flowchart of Real-time Multi-step GA

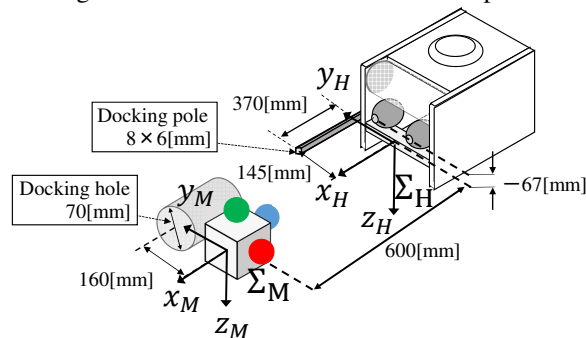


Fig. 3. Coordinate systems of ROV and docking station

3.2 Controller

Because of self stabilization and less effective, roll and pitch angle are neglected in controlling of movement of vehicle. Therefore, 4 DoF (x_d [mm], y_d [mm], z_d [mm] and ϵ_{3d} [deg]) are considered in 3D pose tracking control system. P controller is applied in control system with feedback using estimated pose from 3D model based recognition. The control voltages of four thrusters are calculated by the following proportional control laws.

$$v_1 = k_{p1}(x_d - x) + 2.5 \quad (1)$$

$$v_2 = k_{p2}(\epsilon_{3d} - \epsilon_3) + 2.5 \quad (2)$$

$$v_3 = k_{p3}(y_d - y) + 2.5 \quad (3)$$

$$v_4 = k_{p4}(z_d - z) + 2.5 \quad (4)$$

$$\begin{aligned} x_d &= {}^H x_M = 600 \text{ (350)}[mm], \\ y_d &= {}^H y_M = 12 \text{ (12)}[mm], \\ z_d &= {}^H z_M = -70 \text{ (-70)}[mm], \quad \epsilon_{3d} = 0 \text{ (0)}[deg] \end{aligned}$$

Where x_d , y_d , ϵ_{3d} and z_d are desired relative value based on Σ_H against 3D marker (Fig.3), and v_1 , v_3 and v_4 are the

voltages for thrust of x-axis, y-axis and z-axis direction respectively. ϵ_{3d} stands for rotation angle around z-axis. v_2 means the voltage for torque around z-axis. According to the thruster characteristics which is configured to stop for 2.5 [V], the output voltages for thrust is the differentiated value gained by proportional gain value and added by offset value of 2.5. Based on experimental results, gain coefficients are tuned to have better performance in virtual servoing.

4 EXPERIMENTAL ENVIRONMENT

This experiment was conducted in Hirokawa Town, Aritagun, Wakayama Prefecture, around 2 pm on December 16, 2015. The water depth was about 3.5 [m] and the weather was cloudy. There were some gentle waves while conducting experiments. The layout of a target object(3D marker), docking hole and ROV viewed from above is shown in the Fig.4. ROV was connected by a cable with 200 [m] length to the onshore platform. 3D marker and the docking hole shown in Fig.5 are fixed on the bottom of the structure shown in Fig.6, and it is placed at a depth of about 3 [m]. 3D marker is consisted of three spheres(40[mm] in diameter) whose colors are red, green and blue as shown in Fig.5. Diameter of the docking hole is 70 [mm], and distance between center of 3D marker and hole is 160 [mm]. Fig.6 shows a structure of docking station including the docking hole, 3D marker, and underwater cameras for recording in water.

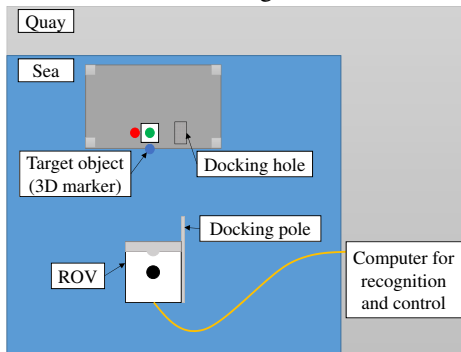


Fig. 4. Layout of docking experiment (top view)

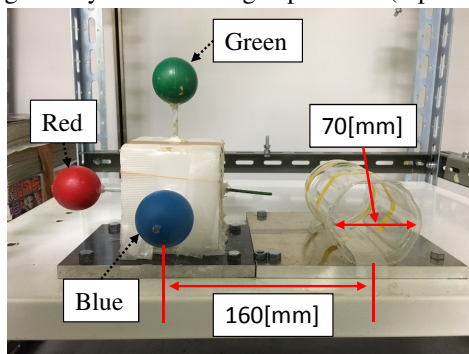


Fig. 5. Docking hole and 3D marker

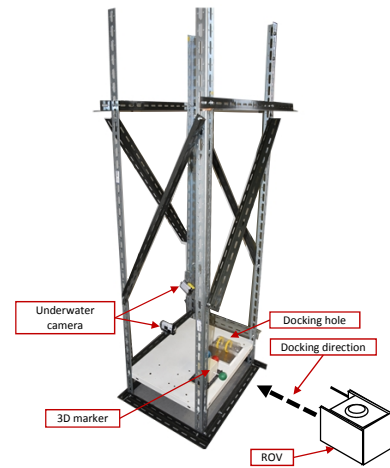


Fig. 6. Structure of docking station

5 DOCKING PROCEDURE

Docking procedure is designed as shown in Fig.7. There are four steps that consist of (a)Approaching, (b)Visual Servoing, (c)Docking and (d)Docking Completion to complete docking operation.

(a) Approaching

Normally, this step is performed using long distance navigation sensor unit. In this work, the vehicle was controlled by manually to approach the docking station till 3D marker was detected by proposed system. By switching from manual operation to automatic control, the state shifts to (b)Visual Servoing.

(b) Visual Servoing

After detecting the 3D marker, relative pose between ROV and 3D marker is estimated using vision based recognition with dual-eye camera. Using estimated pose, ROV are controlled automatically to follow the desired relative pose($x_d = 600$ [mm], $y_d = 12$ [mm], $z_d = -70$ [mm], $\epsilon_{3d} = 0$). When ROV moves to the front of 3D marker and be stable, the state shifts to (c)Docking.

(c) Docking

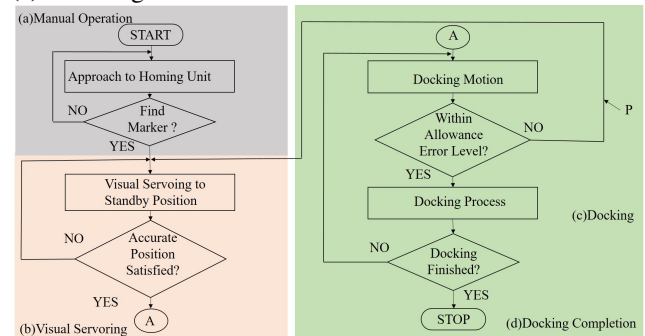


Fig. 7. Flowchart of docking strategy

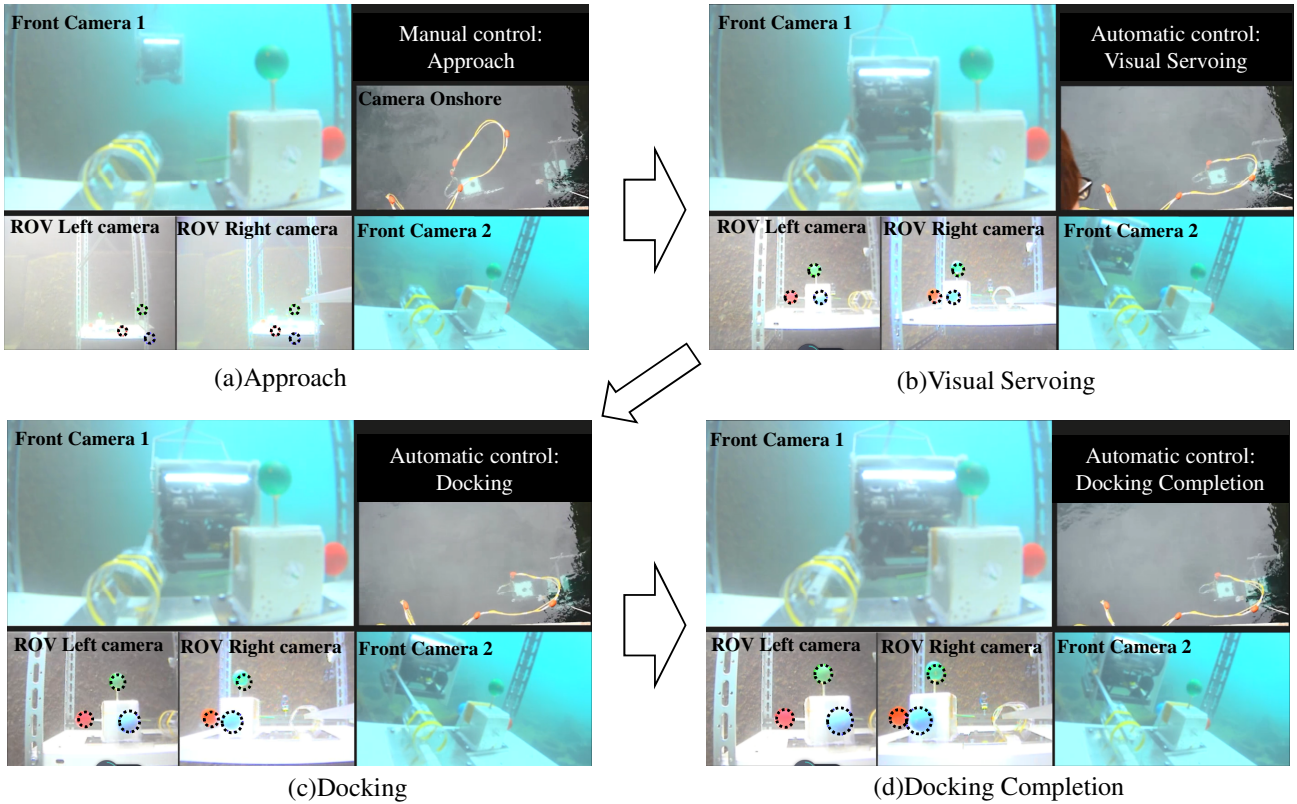


Fig. 9. Docking control sequences by dual-eye visual servoing consisting of (a)Approach by manual operation, (b)Preparation for docking that controls the pose of the vehicle to be constant desired values, (c)Docking by decreasing desired position between 3D marker and the vehicle, (d)completion of docking. Front Camera1 and front Camera2 are photos taken by cameras set at docking frame shown in Fig.6. The photos of ROV Left camera and ROV Right camera are shown in left bottom part of the group photos, with dotted circles indicating real time pose tracking results, and the photo of camera onshore shows the vehicle seen on the quay.

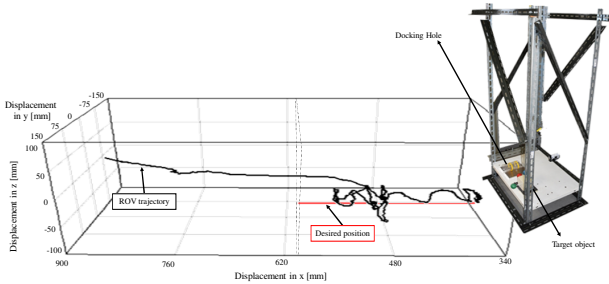


Fig. 8. Position trajectory during docking trial
 When the vehicle is stable with position error of ± 20 [mm] in image plane (y,z) for 165 [ms], the vehicle goes ahead to insert the docking pole into the docking hole decreasing the distance between vehicle and target in x-axis direction gradually until it reaches 350 [mm]. Whenever the relative pose error exceeds allowance range, the process switches to the visual servoing as shown as P in Fig.7.

(d) Docking Completion

This state means docking is completed. ROV is automatically controlled to follow a constant desired relative pose ($x_d = 350$ [mm], $y_d = 12$ [mm], $z_d = -70$ [mm], $\epsilon_{3d} = 0$) as in (b)Visual Servoing.

6 SEA DOCKING EXPERIMENT

Docking tests began with the vehicle in front of dock with distance of 3.5 [m] from the dock. The buoyancy force was nearly 1.03 times than that of fresh water. For demonstration of underwater battery recharging, docking pole attached on vehicle and docking hole fixed with 3D marker was designed as shown in Fig.3. Therefore, the main task is to insert docking pole into the docking hole automatically controlling the vehicle by visual servoing.

6.1 Doking result

Docking results are shown in Fig.8-10. Fig.8 shows position trajectory during docking process. Black line stands for the estimated relative pose between ROV and 3D marker

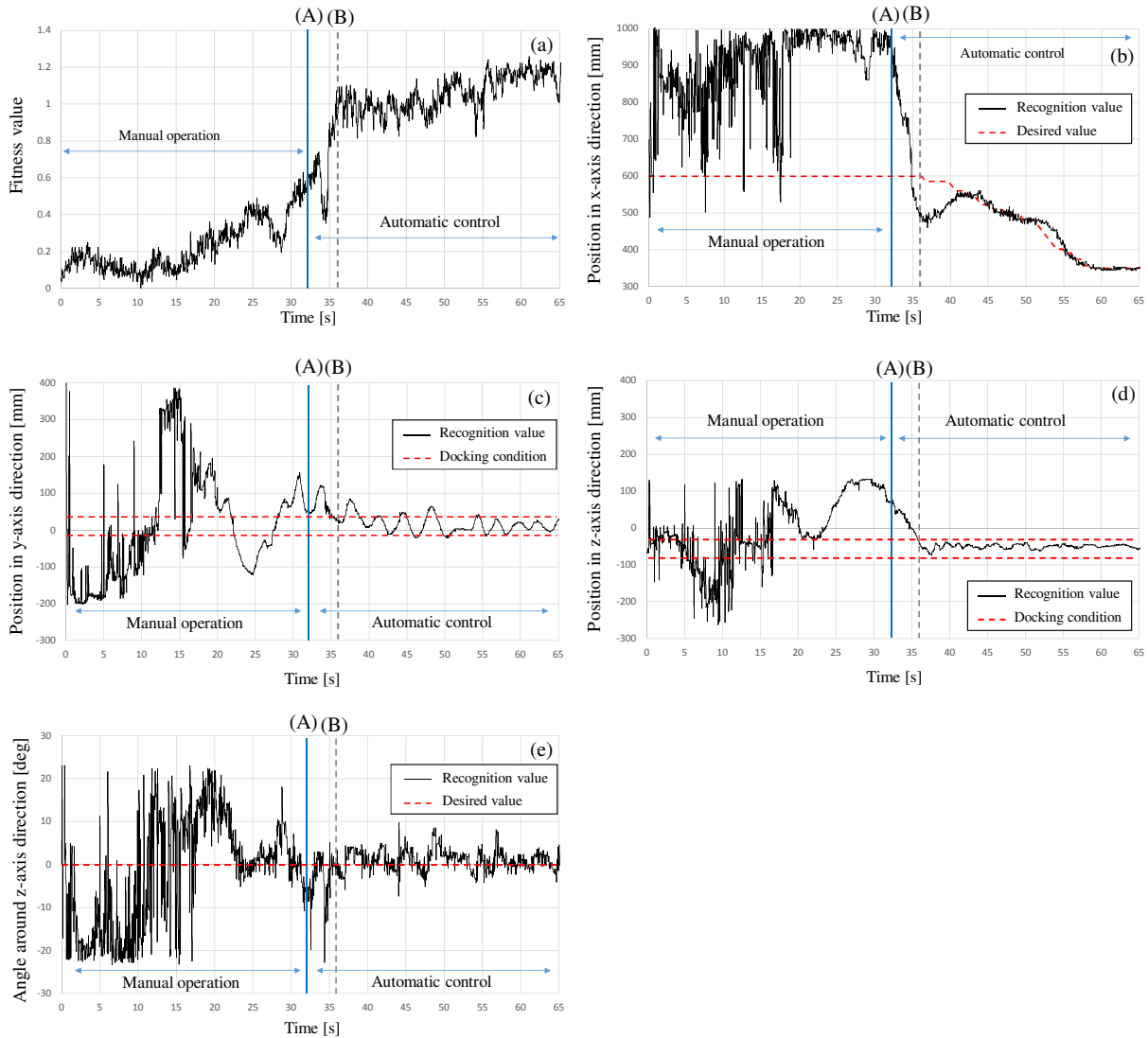


Fig. 10. Docking result : Time profile of (a)fitness value, (b)(c)(d)recognized positions in x,y,z axis direction and (e)angle around z-axis

in the section from (b)Visual Servoing to (d)Docking Completion. Red line stands for the desired position($x_d:600-350$ [mm], $y_d=12$ [mm], $z_d=-70$ [mm], $\epsilon_{3d}=0$) during docking experiment. Fig.9 shows docking steps while conducting sea trial, Fig.9(a)-(d) correspond to the respective states of the docking procedure described in section 5. Fig.9(a) is a state in which ROV is searching the 3D marker while approaching to recharging station by manual operation. At this time, it can be confirmed that the recognized position displayed with the broken line in left and right camera images does not coincide with 3D marker. It means that recognition value is not truthful. Fig.9(b) is a visual servo state. Fig.9(c) shows a state of docking, Fig.9(d) shows a state of docking completion. From these images, it can be seen that docking pole is in the hole and docking operation is completed. Fig.10 shows results of

3D recognition during docking trial. Time profile of fitness value is shown in Fig.10(a). Recognized positions in x, y, and z axis are illustrated in Fig.10(b)-(d). Recognized posture around z axis is illustrated in Fig.10(e). After confirming that fitness value has increased to about 0.6((A) shown in Fig.10(a)), operator manually switched from manual operation to automatic control. After switching, automatic docking is performed according to the flowchart shown in Fig.7. Firstly, ROV moved to the desired relative pose. When the range of control error in image plane ($|y_d - y|$ and $|z_d - z|$) is within ± 20 [mm] for 165 [ms], the docking pole docks into the hole by decreasing desired value(x_d) with the velocity of 30 [mm/s] until it reaches 350 [mm]. It can be seen that docking step was performed when the position errors in y-axis and z-axis were within predefined range ($-8 < y < 32$

and $-9 < z < -50$) written in red dotted lines as shown in Fig.10(c), (d). There is a situation that the position in y-axis deviates from the docking condition after 36 [s] (shown in Fig.10). In this case, docking step shifts to (b) Visual Servoing via P route in Fig.7. Furthermore, it can be seen that rotation error around z-axis shows less than ± 10 [deg] during docking. It can be confirmed that the docking operation was success within 40 [s] after starting automatic control. As a result, it can be said that successful sea docking was conducted using proposed system.

7 CONCLUSION

We have been studying docking work to achieve long-term activity of underwater vehicle in actual sea area. According to the experimental results, docking operation using dual-eye vision based recognition was successfully conducted with enough accuracy. Docking trial with an actual AUV in sea is our future work.

ACKNOWLEDGMENT

This work is supported in part by KOWA corporation for the development of ROV.

REFERENCES

- [1] Feihu Sun, Junzhi Yu and De Xu, "Visual Measurement and Control for Underwater Robots: A Survey", *25th Control and Decision Conference (CCDC)*, pp.333-338, 2013.
- [2] J.-Y. Park, B.-H. Jun, P.-M. Lee, and J. Oh, "Experiments on vision guided docking of an autonomous underwater vehicle using one camera", *Ocean Engineering*, vol. 36, no. 1, pp. 48-61, Jan. 2009.
- [3] Ura. T. Kurimoto, Y., Kondo, H., Nose, Y. Sakamaki, T. and Kuroda, Y., "Observation behavior of an AUV for ship wreck investigation", *Proceedings of the OCEANS 2005 MTS/IEEE*, Vol.3, pp.2686-2691, 2005.
- [4] Palomeras, N., Ridao, P., Ribas, D. and Vallicrosa, G., "Autonomous I-AUV docking for fixed-based manipulation", *Preprints of the International Federation of Automatic Control*, pp.12160-12165, 2014.
- [5] Ken Teo, E. An, and P.-P. J. Beaujean, "A robust fuzzy autonomous underwater vehicle (AUV) docking approach for unknown current disturbances", *IEEE Journal of Oceanic Engineering*, Vol.37, no.2, pp. 143-155, April 2012.
- [6] Amaury N'egre, C edric Pradalier, Matthew Dunbabin, "Robust vision-based underwater homing using self similar landmarks", *Journal of Field Robotics, Wiley-Blackwell, Special Issue on Field and Service Robotics*, vol.25(6-7), pp.360-377, 2008.
- [7] Myo Myint, Kenta YONEMORI, Akira YANOU, Shintaro ISHIYAMA and Mamoru MINAMI, "Robustness of Visual-Servo against Air Bubble Disturbance of Underwater Vehicle System Using Three-Dimensional Marker and Dual-Eye Cameras", *OCEANS 2015. MTS/IEEE Conference and Exhibition*, 2015.
- [8] Myo Myint, Kenta Yonemori, Akira Yanou, Khin Nwe Lwin, Mamoru Minami and Shintaro Ishiyama, "Visual Servoing for Underwater Vehicle Using Dual-eyes Evolutionary Real-time Pose Tracking", *Journal of Robotics and Mechatronics*, Vol.28, No.4, 2016.
- [9] Yanou, A., Ohnishi, S., Ishiyama, S. and Minami, M., "Autonomous docking control of visual-servo type underwater vehicle system aiming at underwater automatic charging", *Transactions of the JSME*, Vol.81, No.832, pp.15-00391, 2015.
- [10] Yu F., Minami M., Song W., Zhu J. and Yanou A., "On-line head pose estimation with binocular hand-eye robot based on evolutionary model-based matching", *Journal of Computer and Information Technology*, Vol.2, No.1, pp.43-54, 2012.